

Document downloaded from:

<http://hdl.handle.net/10251/37698>

This paper must be cited as:

Trujillo Guillen, M.; Ribera, V.; Quesada, R.; Berjano, E. (2012). Applicator for RF Thermokeratoplasty: Feasibility Study Using Theoretical Modeling and Ex Vivo Experiments. *Annals of Biomedical Engineering*. 40(5):1182-1191. doi:10.1007/s10439-011-0492-1.



The final publication is available at

<http://dx.doi.org/10.1007/s10439-011-0492-1>

Copyright Springer Verlag (Germany)

NOTE

Circular applicator with suction ring for radiofrequency heating of the cornea: feasibility study using theoretical modeling and ex vivo experiments

Macarena Trujillo¹, Vicente Ribera², Rita Quesada³, Enrique Berjano⁴

¹Instituto Universitario de Matemática Pura y Aplicada, Universitat Politècnica de València, Spain

² Neptury Technologies, Almassora, Spain

³ Department of Surgery, Hospital del Mar, Barcelona, Spain

⁴ Biomedical Synergy, Electronic Engineering Department, Universitat Politècnica de València, Spain

*To whom all correspondence should be addressed:

Dr. Enrique Berjano

Biomedical Synergy, Electronic Engineering Department (7F)

Universitat Politècnica de València, Spain

Camino de Vera, 46022 Valencia, Spain

Phone: 34–963877607 Fax: 34–963877609

Email: eberjano@eln.upv.es

Abstract

Radiofrequency (RF) thermokeratoplasty (RF-TKP) uses RF currents to alter the curvature of the cornea by means of thermal lesions. We built an RF applicator which combined a microkeratome suction ring and a circular electrode with the aim of creating circular thermal lesions in a predictable, uniform and safe way. An experimental study was conducted on *ex vivo* porcine eyes to assess both the electrical performance and the histological characteristics of the lesions. We also designed a theoretical model to study the electrical-thermal phenomena involved in the RF heating of the applicator. The experimental results showed a lesion depth of $34.2 \pm 11.0\%$ of corneal thickness with 200 μm electrode at a constant voltage of 50 V up to roll-off (1000 Ω of impedance). With a voltage of 30 V for 30 s the mean depth was $36.8 \pm 8.1\%$. The progress of electrical impedance throughout heating and lesion dimensions were used to compare the experimental and theoretical results. The evolution of impedance obtained from the theoretical model showed good agreement with that obtained in the experiments. The lesion dimensions computed from the theoretical model were around twice the size of those obtained from the experiments. Despite this disagreement, the effect of changing voltage and time (experimental Group) on the thermal dimensions showed the same tendency in theoretical and experimental models. This could have been due to the parameters chosen in the formulation of the thermal damage model. The findings suggest that the 200 μm electrode could be a suitable option for creating uniform circular thermal lesions, such as those required to correct hyperopia.

Keywords: Conductive keratoplasty, cornea, *ex vivo* experiments, ophthalmology, radiofrequency heating, theoretical modeling, thermokeratoplasty

1. Introduction

The radiofrequency (RF) thermokeratoplasty (RF-TKP) technique was proposed in 1980 to reshape cornea curvature by means of thermal lesions using RF currents (≈ 500 kHz) (Doss and Albillar 1980). The temperature of the corneal stroma is raised to achieve the irreversible shrinkage of collagen fibers. By using a particular lesion pattern it is possible to change the corneal curvature in a controlled way and therefore to correct refractive errors such as hyperopia (Pallikaris *et al* 2005), presbyopia (Stahl 2007) and astigmatism (Alió *et al* 2005). Hyperopia correction implies creating a circular pattern (6-8 mm diameter) of lesions in the cornea. This surgical procedure, known currently as *conductive keratoplasty* (CK), is conducted by means of a hand-held instrument which includes a needle-like RF microelectrode (length 450 μm and width 90 μm) (Berjano *et al* 2007), which is introduced into the cornea to create thermal spots. Although some studies have demonstrated that CK is an effective and safe treatment, recent studies have reported both significant regression of refractive effects over an extended follow-up period (Moshirfar *et al* 2005) and poor predictability (Xu *et al* 2010). Furthermore, serious problems such as corneal perforation (Kymionis *et al* 2003, Ou and Manche 2007) and anterior chamber inflammation (Ehrlich and Manche 2009) have also been reported. It therefore seems that an effort should be made to improve RF-TKP techniques. Our group proposed a ring electrode for RF-TKP in 2003 (Berjano *et al* 2003) with the idea of developing an applicator capable of creating a complete circular lesion pattern, as opposed to the single-spot pattern obtained by CK. The rationale of this hypothetical benefit was the enormous potential of circular fully thermal lesions (previously created with heated brass rings) to increase corneal refracting power by up to 14 diopters (Gruenberg 1981, Miller and Manning 1978). In our dosimetry study on enucleated rabbit eyes, the histological analyses showed a non-uniform lesion along the circular path, probably due to non-uniformity of the electrode-tissue contact. In fact, this is also a potential

problem with CK, in which the surgeon inserts the electrode manually and hence there could be differences between the created spots. In order to minimize the effect of this parameter as far as possible, we now propose a new design of RF applicator in order to obtain uniform electrode-cornea contact throughout the contact area and to spatially homogenize the electrical-thermal phenomena.

In order to achieve the necessary stability and precision involved in corneal microkeratome, we combined the suction ring of a microkeratome with a circular microelectrode to develop a new RF-TKP applicator with the goal of creating circular thermal lesions in a predictable, uniform and safe way. We first built an applicator and then planned an experimental study on *ex vivo* porcine eyes to assess both the electrical performance and the histological characteristics of the lesions. Finally, we built a theoretical model to study the electrical-thermal phenomena involved in RF heating with this applicator. The progress of electrical impedance throughout heating and the dimensions of the created thermal lesions were used to compare the experimental and theoretical results.

2. Materials and methods

2.1. Experimental study

The applicator is a prototype based on a circular electrode embedded in an epoxy plane. This element was placed in a microkeratome Hexatome (Neptury Technologies, Almassora, Spain) exactly where the blade is usually located. We built two 7-mm diameter circular electrodes with thicknesses of 100 μm and 200 μm , respectively (see Fig. 1). The electrode was made of 316L stainless steel and was inserted it into an epoxy plane of a standard microkeratome. Finally, this epoxy plane was placed in the head of the microkeratome as shown in Fig. 2.

The experimental model was based on enucleated porcine eyes, which were obtained eight hours *post mortem* and stored in a cold saline solution at 5°C to minimize swelling and

autolysis. Prior to RF application, the adjacent tissue was removed and saline was injected by syringe into the ocular globe to achieve a suitable stiffness. The eyes were then placed in a custom-made holder and held in place by the applicator itself. The experiments were conducted using a RF generator CC-1 Cosman Coagulator System (Radionics, Burlington, MA, USA), which delivers a non modulated sinusoid waveform up to 100 V (rms) on 100 Ω and with a maximum current of 1 A. The electrical impedance, current, voltage and power were recorded in a computer (sampling frequency of 30 Hz). In this RF generator, the user sets the output voltage (without load), along with the heating duration. In addition, since the electrical impedance is continuously measured, there is an automatic switch-off mode once the impedance passes 1 k Ω . This phenomenon is called roll-off, and is associated with a high degree of desiccation of the tissue. At this time, the higher the RF power applied, the higher the risk of arcing and tissue disruption. Roll-off could thus be considered as a method of increasing safety. In all the experiments the built-in suction ring of the microkeratome acts as a dispersive electrode.

As this was the first thermal dosimetry bench-study, the experimental groups were tentatively chosen in order to achieve sufficiently-deep thermal lesions, i.e. around 50% of corneal thickness. We considered six experimental groups, three for each electrode thickness, and five eyes per group, i.e. a total of thirty eyes. Two eyes were used as a control to check the status of the samples provided, and two further eyes were used as a second control to analyze the simple effect of placing the electrode on the cornea (i.e. without applying RF power). The characteristics of each experimental group are shown in Table 1. There were three groups (1, 2 and 4) in which we set a constant voltage up to roll-off, since this approach had been previously employed in other RF heating techniques (Arata *et al* 2001). However, when the set voltage was low, e.g. 20 V with the 100 μm electrode, it was not possible to reach roll-off, and so the time was fixed at 60 s (Group 3). Since the area of the 200 μm

electrode is obviously larger than the 100 μm , it was even more difficult to reach roll-off with 30 V, so that Groups 5 and 6 were programmed with fixed times of 30 and 60 s duration. As a result,

The study was divided into two parts: a histological analysis of the heated corneas and an analysis of the progress of the electrical impedance during RF heating. The histological analysis was based on 4 μm -thick slices stained with hematoxylin and eosin (H&E). Each cornea was transversally cut to identify the lesion geometry in both sides. The thermal lesion was assessed by the coagulation contour characterized by a more intense pigmentation. The lesion geometry was quantified by two variables: depth (maximum value reached at the center) and width (measured on the cornea surface). Both variables were expressed as a percentage of corneal thickness.

2.2. Theoretical model

The problem was based on a coupled electric-thermal problem, which was solved numerically using the Finite Element Method (FEM) by means of COMSOL Multiphysics software (Comsol Inc., Burlington, MA, USA). The geometry and the dimensions of the theoretical model are shown in Fig. 3. Due to the geometry, the problem presented axial symmetry and a two-dimensional (2D) analysis could be conducted. The model included a fragment of cornea, aqueous humor, and metallic electrode embedded in epoxy (plastic plane). For the theoretical modeling we only considered the 200 μm electrode, since this showed satisfactory results (see Results Section). The dispersive electrode was modeled as an electrical condition on boundaries at a distance from the active electrode. We considered a flat geometry of the cornea. Although the inclusion of curvature of the cornea in the theoretical modeling could modify the computed temperature distributions (Berjano *et al* 2002), the suction pressure in the new applicator keeps the cornea totally flat, and hence the model geometry is suitable.

The dimensions R and Q were estimated by means of a sensibility analysis in order to avoid boundary effects. We used the value of the maximum temperature (T_{\max}) reached in the cornea after 5 s of RF heating at 50 V as a control parameter in these analyses. The value of the parameters was increased by equal amounts in each simulation. When there was a difference of less than 0.5% between T_{\max} and the same parameter in the previous simulation, we considered the former values as appropriate. The characteristics of the materials and tissues used in the model are shown in Table 2 (Berjano *et al* 2006, Jo and Aksan, 2010). The electrical and thermal conductivity of the cornea were temperature-dependent, as defined in Jo and Aksan (2010). For the thermal conductivity (k) we considered linear growth of +0.26%/°C up to 100°C, and then k was kept constant. The electrical conductivity (σ) grew exponentially +1.7%/°C up to 100°C, between 100 and 105°C was constant and then σ decreased linearly by approximately 2 orders for five degrees. From a mathematical point of view the model was based on a coupled electric-thermal problem. In the tissue, the governing equation for the thermal problem was the Bioheat Equation (Berjano 2006):

$$\rho c \frac{\partial T}{\partial t} = \nabla(k\nabla T) + q + Q_p + Q_m \quad (1)$$

where T is temperature, t is time, ρ is density, c is specific heat, k is thermal conductivity, q is the heat source produced by RF power, Q_p is heat loss from blood perfusion and Q_m is metabolic heat generation. Q_p and Q_m are insignificant in RF-TKP and thus were not considered. The heat source q (Joule losses) is given by $q=JE$, where J is current density and E is electric field strength. Both were obtained from the electrical problem. The governing equation for the electrical problem is the Laplace equation $\nabla^2 V=0$, where V is the voltage. The electric field E is calculated by means of $E = -\nabla V$ and current density J using Ohm's law ($J= \sigma E$). We used a quasi-static approach due to the frequencies used in RF-TKP (≈ 500 kHz) and for the geometric area of interest the tissues can be considered as purely resistive. Tissue

vaporization was modeled by modifying Equation (1) according to (Abraham and Sparrow 2007). The product density×specific heat of the cornea in the liquid and gas phases were $4.06\times 10^6 \text{ J/K}\cdot\text{m}^3$ and $2\times 10^6 \text{ J/K}\cdot\text{m}^3$ respectively, while the product at the phase change was $3.7\times 10^8 \text{ J/K}\cdot\text{m}^3$ (Jo and Aksan 2010). The enthalpy of transition associated with collagen denaturation was not considered, since its effect is insignificant compared to the effects of tissue vaporization (Jo and Aksan 2010).

The electrical boundary conditions were: zero current density in the transversal direction to the symmetry axis, at air-plastic interface, and at the outer end of the aqueous humor. Zero voltage was set in the dispersive electrode. Since we modeled only the cases corresponding to the experimental Groups 4 and 5 (see Results section), the voltage applied by the electrode was modeled as a point source at the electrode of value 30 (Group 5) or 50 V (Group 4). The performance of the RF generator used in the experiments required a manual increase from 0 V to the target voltage. In this respect, we estimated that during the experiments the increase in applied voltage could last for up to 1 s. We therefore included a linear increase in the applied voltage in the simulations with duration of 1 s (between 0 and 50 V). The thermal boundary conditions were: null thermal flux in the transversal direction to the symmetry axis, constant 21°C (room temperature) in the dispersive electrode and at the outer end of the aqueous humor. The air circulating around the plastic plane and the aqueous humor circulating under the cornea produce a cooling effect on the plastic and cornea surfaces, modeled by means of two thermal convection coefficients h_1 and h_2 , respectively. We considered values of $h_1 = 20 \text{ W/m}^2\text{K}$, and $h_2 = 500 \text{ W/m}^2\text{K}$ (Berjano *et al* 2002). The initial temperature was set at 21°C. The mesh was heterogeneous, with a mesh size of 25 μm around the electrode-tissue interface where the highest gradient was expected. The size of the finer mesh was estimated by means of a sensibility analysis following the same steps as in the case of the parameters R and Q. For the time-step in the solver we used shorter times at the

beginning of the heating process, when sudden changes in temperature and voltage could be expected.

The damage to tissue due to heating is a function of the temperature increase and the exposure time (Henriques 1947, Miller and Ziskin 1989). The thermal damage geometry was obtained by means of the Arrhenius damage model (Pearce *et al* 2005):

$$\Omega(\tau) = A \int_0^{\tau} e^{-\frac{\Delta E}{RT(t)}} dt \quad (2)$$

where Ω is the thermal damage accumulated during heating, A (s^{-1}) is the frequency factor, ΔE (J/mol) is the activation energy, and R the gas constant (8.314 J/mol·K). Both A and ΔE are kinetic coefficients evaluated for each tissue type from experimental data. For the cornea we used $A=1.61 \times 10^{45} s^{-1}$ and $\Delta E=3.06 \times 10^5$ J/mol (Pearce *et al* 2005). The depth and surface width of the lesions (expressed as percentage of corneal thickness) were computed from the line $\Omega=1.0$ and then compared to experimental lesions.

3. Results

3.1. Experimental results

In general, in Groups 1, 2 and 3 (100 μm electrode) it was hard to find apparent lesions. Only in one sample of Group 1 was a very superficial lesion found (see Fig. 4). In contrast, the 200 μm electrode created sizeable thermal lesions (Groups 4, 5 and 6). In Group 4 (50 V voltage up to roll-off), although it was not possible to photograph the entire cornea (i.e. showing the lesions on both sides), we observed that lesions were uniform along the circular path in the five samples (see Fig. 5). The time to roll-off was 4.5 ± 0.9 s. The lesion depth and width were $34.2 \pm 11.0\%$ and $56.2 \pm 5.7\%$ respectively. We also found a strong inverse linear relationship between initial impedance and lesion depth ($R^2= 92.2\%$). Fig. 6A shows the evolution of

impedance, which was similar for all samples: a slow initial decrease was followed by a sudden increase up to a value between 500 and 800 Ω , and then a more or less continuous increase up to roll-off (1000 Ω).

Lesion depth and width in Group 5 were $36.8\pm 8.1\%$ and $57.0\pm 12.5\%$ respectively. In contrast to Group 4, in Group 5 we found large differences in the lesion depth along the intra-sample circular path, in some cases, up to 46% of corneal thickness. Fig. 7A shows the evolution of impedance in this group. In all cases there was a short initial reduction followed by a sudden rise up to a value between 300 and 600 Ω , and then a more or less continuous increase but never reaching roll-off. Finally, in Group 6 the lesion depth and width were $34.8\pm 8.9\%$ and $63.4\pm 21.3\%$ respectively. The high dispersion in lesion width was due to the lesion spreading over the cornea surface during the long heating period in some cases.

3.2. Theoretical modeling results

In this part of the study we modeled the cases from experimental Groups 4 and 5, as they showed promising results from the clinical application point of view. We obtained the model dimensions $R=3.5$ mm and $Q=5$ mm from the sensitivity analysis (see Fig. 3). Fig. 6B and 7B shows the computed impedance evolution corresponding to Groups 4 and 5 respectively. We observed a gradual initial decrease followed by a sudden increase up to a certain value, followed by a more or less continuous increase, which indicates similar behavior in both the experimental and theoretical results.

Fig. 8 shows the temperature distributions during RF heating at 50 V up to roll-off (similar conditions to experimental Group 4). One of the findings was the preferential heating at the outer edge of the electrode (between 0.4 and 0.6 in Fig. 8). At the roll-off time (5 s) the lesion depth and width were 53.7% and 108.0% of corneal thickness respectively (see solid $\Omega=1.0$ in Fig. 8). Fig. 9 shows the temperature distributions during RF heating at 30 V for 30

s (similar conditions to experimental Group 5). Here also there was preferential heating at the outer edge of the electrode (at 1.0 s in Fig. 9). At the end of the heating period (30 s) lesion depth and width were 60.5% and 124.0% of corneal thickness, respectively (see solid $\Omega=1.0$ in Fig. 9).

4. Discussion

The objective of this study was to assess the feasibility of using a RF applicator to heat the cornea following a circular pattern as nearly homogeneous as possible. To this end we built an applicator combining a microkeratome vacuum ring with a circular electrode embedded in the epoxy plane, which contains the blade in a standard microkeratome. We then designed an experimental dosimetry study based on excised porcine eyes, measuring the geometry of the thermal lesions and the evolution of impedance throughout the process. Due to the impossibility of accurately mapping intracorneal temperatures (e.g. by means of thermocouples), we developed a theoretical model to study temperature distribution in the cornea during heating. Impedance progress and lesion dimensions were used to compare experimental and theoretical results and thus to experimentally validate the theoretical models.

The experimental results showed that the 100 μm electrode was not able to create such deep lesions as the 200 μm electrode. This seems logical, since there is a direct relationship between electrode size and lesion depth (Haines *et al* 1990). It is also reasonable to expect roll-off only in Group 4 since a higher level of applied voltage (50 V) was used here than in the other groups (30 V).

It is interesting to note the inverse linear relationship between initial impedance and lesion depth in this group ($R^2= 92.2\%$), which was not found in the other groups. This could be due to the heating period in Group 4 being short enough (4.5 s) to avoid the thermal

conduction phenomenon affecting thermal lesions, as opposed to the long times (30 and 60 s) used in Groups 5 and 6. In other words, the thermal lesion was created almost entirely by the applied power density (W/kg), also known as *Specific Absorption Rate* (SAR). This was due to setting a constant voltage, which meant that lower initial impedance implied a higher electrical current and hence a higher power level. In contrast, this did not occur in Groups 5 and 6, in which the longer heating time caused thermal conduction to affect the thermal lesions. Additionally, these results confirm that intrinsic dispersion of tissue characteristics has a greater influence on lesion size in longer heating periods (Berjano *et al* 2002). Also interesting is the low dispersion found in Group 4 lesion width. Similar behavior had been observed in a previous study (Berjano *et al* 2002), in which two groups of corneas were heated by RF currents for 1 s using two levels of applied voltage (16 and 21 V). In that study, lesion depth was very different for the 2 groups ($21\pm 1\%$ vs. $30\pm 4\%$ of corneal thickness), whereas width was similar ($106\pm 7\%$ vs. $108\pm 9\%$). By taking all these results into account, we can conclude that for short heating periods (< 5 s), lesion depth is highly related to initial impedance and applied voltage (Berjano *et al* 2002), whereas lesion width could be less dependent on those factors and perhaps more closely related to electrode size.

From a practical point of view, the experimental results suggest that the applicator based on the 200 μm electrode, in conjunction with the RF power-delivering protocol as used in Group 4, could be a suitable option for creating thermal lesions such as those required to correct hyperopia. Note that (Table 3) initial impedances around 100 Ω could create thermal lesions with a depth close to 50% of corneal thickness). In fact, since it has been shown to create a uniform circular thermal lesion, it could both improve the predictability of the current intra-stromal microelectrodes and achieve improved refractive changes.

We chose the option of comparing the evolution of electrical impedance during heating in the experimental and computational results due to the impossibility of obtaining accurate

measurements by inserting micro-thermocouples into the cornea and mapping the temperature profile (Berjano *et al* 2005). In our study we found a good agreement between theoretical and experimental results regarding the impedance progress (see Figures 6 and 7).

Table 4 shows the results for Groups 4 and 5 of a comparison of lesion sizes obtained from histological analysis and theoretical modeling. The lesion dimensions computed from the theoretical model were around twice the size of those obtained from the experiments. In spite of this disagreement, the effect of changing voltage and time (experimental Group) on the thermal dimensions showed the same tendency in theoretical and experimental models. This could be due to the fact that the A and ΔE parameters used in the formulation of the thermal damage model correspond with the birefringence loss in the coagulated tissue (Pearce *et al* 2005), whereas the H&E color change boundary was used to assess the experimental lesions. This makes sense, as the loss of birefringence occurs at lower temperatures than other histological markers (Thomsen *et al* 1989).

By comparing Figures 6B and 8, we notice that the initial heating (lower than 100°C) corresponds with the initial decrease in impedance. Once the temperature reaches 100°C at some point in the tissue, electrical conductivity suddenly drops and impedance steeply increases (0.6 s in Fig. 6B). When the entire electrode is totally surrounded by dehydrated tissue (i.e. heated over 100°C), the abrupt increase ceases and from this time on impedance gradually increases. This last phenomenon is associated with a considerable heat flux from tissue to electrode (from 3.5 to 5 s in Fig. 8). Similar behavior can be inferred from Figures 7B and 9 (case of 30 V for 30 s).

This study has certain limitations. Firstly, the experimental method used to assess lesion dimensions was routine light microscopy, which does not allow high-resolution observation of some morphological changes, as opposed to other techniques such as transmission polarizing microscopy (Thomsen *et al* 1989). Secondly, the parameters A and ΔE used in the

formulation of the thermal damage model correspond with birefringence loss in coagulated tissue (Pearce *et al* 2005). We do not know the precise relationship between the onset of this process and the pigmentation observed after staining with H&E. And thirdly, the experimental results are based on excised tissue and hence the findings have to be confirmed in *in vivo* models to assess the mid-term topographic and refractive changes.

5. Conclusions

Our experimental findings suggest that: 1) The applicator based on a 200 μm electrode allows perfectly circular thermal lesions to be created with a depth close to 50% of corneal thickness, by using a constant voltage of 50 V until roll-off; 2) longer times with lower voltages produce non uniform lesions along the circular path; and 3) the applicator based on a 100 μm electrode is not able to create significant lesions. The evolution of electrical impedance throughout heating obtained from the computer simulations showed good agreement with those obtained from the experimental studies.

Acknowledgements

This work received financial support from the Spanish “Plan Nacional de I+D+I del Ministerio de Ciencia e Innovación” Grant No. TEC2008-01369/TEC and FEDER Project MTM2010-14909. The translation of this paper was funded by the Universitat Politècnica de València, Spain

References

- Abraham J P and Sparrow E M 2007 A thermal-ablation bioheat model including liquid-to-vapor phase change, pressure- and necrosis-dependent perfusion, and moisture-dependent properties *Int J Heat Mass Tran* 2007. **50** 2537–44
- Alió JL, Ramzy MI, Galal A and Claramonte PJ 2005 Conductive keratoplasty for the correction of residual hyperopia after LASIK *J Refract Surg* **21** 698–704
- Arata MA, Nisenbaum HL, Clark TW and Soulen MC 2001 Percutaneous radiofrequency ablation of liver tumors with the LeVeen probe: is roll-off predictive of response? *J Vasc Interv Radiol* **12** 455–8
- Berjano EJ, Saiz J and Ferrero JM 2002 Radio-frequency heating of the cornea: theoretical model and in vitro experiments *IEEE Trans Biomed Eng* **49** 196–205
- Berjano EJ, Saiz J, Alió JL and Ferrero JM 2003 Ring electrode for radio-frequency heating of the cornea: modelling and in vitro experiments *Med Biol Eng Comput* **41** 630–9
- Berjano EJ, Alió JL and Saiz J 2005 Modeling for radio-frequency conductive keratoplasty: implications for the maximum temperature reached in the cornea *Physiol Meas* **26** 157–72
- Berjano EJ 2006 Theoretical modeling for radiofrequency ablation: state-of-the-art and Challenges for the future. *Biomed Eng Online* Apr 18;5:24.
- Berjano E J, Burdío F, Navarro A C, Burdío J M, Güemes A, Aldana O, Ros P, Sousa R, Lozano R, Tejero E and de Gregorio MA 2006 Improved perfusion system for bipolar radiofrequency ablation of liver. *Physiol Meas* **27** N55-N66
- Berjano EJ, Navarro E, Ribera V, Gorris J and Alió JL 2007 Radiofrequency heating of the cornea: an engineering review of electrodes and applicators *Open Biomed Eng J* **1** 71–6
- Doss JD and Albillar JI 1980 A technique for the selective heating of corneal stroma *Contact Intraocular Lens Med* **6** 13–17
- Ehrlich JS and Manche EE 2009 Regression of effect over long-term follow-up of conductive keratoplasty to correct mild to moderate hyperopia *J Cataract Refract Surg* **35** 1591–6
- Gruenberg P, Manning W, Miller D and Olson W 1981 Increase in rabbit corneal curvature by heated ring application *Ann Ophthalmol* **13** 67–70
- Jo B and Aksan A 2010 Prediction of the extent of thermal damage in the cornea during conductive keratoplasty *J Therm Biol* **35** 167–74

- Kymionis GD, Titze P, Markomanolakis MM, Aslanides IM and Pallikaris IG 2003 Corneal perforation after conductive keratoplasty with previous refractive surgery *J Cataract Refract Surg* **29** 2452–4
- Haines DE, Watson DD and Verow AF 1990 Electrode radius predicts lesion radius during radiofrequency energy heating. Validation of a proposed thermodynamic model *Circ Res* **67** 124–9
- Henriques FC 1947 Studies of thermal injury *Arch Pathol* **5** 489–502
- Miller D and Manning WJ 1978 Alterations in curvature of bovine cornea using heated rings *Invest Ophthalmol* **297**
- Miller MW and Ziskin MC 1989 Biological consequences of hyperthermia *Ultrasound Med Biol* **15** 702–22
- Moshirfar M, Feilmeier M and Kumar R 2005 Anterior chamber inflammation induced by conductive keratoplasty *J Cataract Refract Surg* **31** 1676–7
- Ou JI and Manche EE 2007 Corneal perforation after conductive keratoplasty in a patient with previously undiagnosed Sjögren syndrome *Arch Ophthalmol* **125** 1131–2
- Pallikaris IG, Naoumidi TL and Astyrakakis NI 2005 Long-term results of conductive keratoplasty for low to moderate hyperopia *J Cataract Refract Surg* **31** 1520–9
- Pearce J, Panescu D and Thomsen S 2005 Simulation of diopter changes in radio frequency conductive keratoplasty in the cornea *WIT Transactions on Biomedicine and Health* **8** 469–77
- Stahl JE 2007 Conductive keratoplasty for presbyopia: 3-year results *J Refract Surg* **23** 905–10
- Thomsen S, Pearce JA and Cheong WF 1989 Changes in birefringence as markers of thermal damage in tissues *IEEE Trans Biomed Eng* **36** 1174–9
- Xu W, Ye P, Yao K, Ma J and Xu H 2010 Conductive keratoplasty for the treatment of astigmatism induced by corneal trauma or incision *J Refract Surg* **26** 33–42

Table 1 Characteristics of the experimental groups

Group	Electrode thickness (mm)	RF power delivery protocol	
		Voltage	Time
1	0.1	50 V	Up to roll-off
2		30 V	Up to roll-off
3		20 V	60 s
4	0.2	50 V	Up to roll-off
5		30 V	30 s
6		30 V	60 s

Table 2. Characteristics of tissue and materials used in the theoretical model (at 25°C)

Tissue/material	Electrical conductivity (S/m)	Thermal conductivity (W/m·K)	Mass density (kg/m ³)	Specific heat (J/kg·K)
Electrode	7.4×10^6	15	8×10^3	480
Plastic	10^{-5}	0.026	70	1045
Aqueous humour	2.1	0.578	1000	4180
Cornea	$1.12^{(1)}$	0.556	1060	3830

⁽¹⁾ Value chosen to obtain an initial impedance value of 109 Ω , i.e. the mean value found in experimental Group 4.

Table 3. Lesion characteristics of the experimental groups for the 200 μm electrode

Group	Sample	Initial	Lesion ⁽¹⁾		t (s) ⁽²⁾
		impedance (Ω)	Depth (%)	Width (%)	
4	#1	97	40	53	4.8
	#2	95	47	54	5.1
	#3	122	26	60	5.2
	#4	108	38	64	3.1
	#5	124	20	50	4.3
5	#1	109	30	54	
	#2	116	46	53	
	#3	113	30	46	
	#4	135	- ⁽³⁾	- ⁽³⁾	
	#5	169	41	75	
6	#1	170	36	72	
	#2	145	35	60	
	#3	146	46	57	
	#4	166	36	93	
	#5	150	21	35	

⁽¹⁾ Lesion assessed as percentage of corneal thickness.

⁽²⁾ Time (s) up to roll-off for Group 4.

⁽³⁾ Sample missing in histological processing.

Group 4: 50 V up to roll-off; Group 5: 30 V for 30 s; Group 6: 30 V for 60 s.

Table 4. Comparison of experimental and theoretical results of Groups 4 and 5.

		Experimental	Theoretical
Group 4	Time to roll-off (s)	4.5 ± 0.9	5.0
(50 V up to roll-off)	Lesion depth (%)	34.2 ± 11.0	53.7
	Lesion width (%)	56.2 ± 5.7	108.0
Group 5	Lesion depth (%)	36.8 ± 8.1	60.5
(30 V for 30 s)	Lesion width (%)	57.0 ± 12.5	124.0

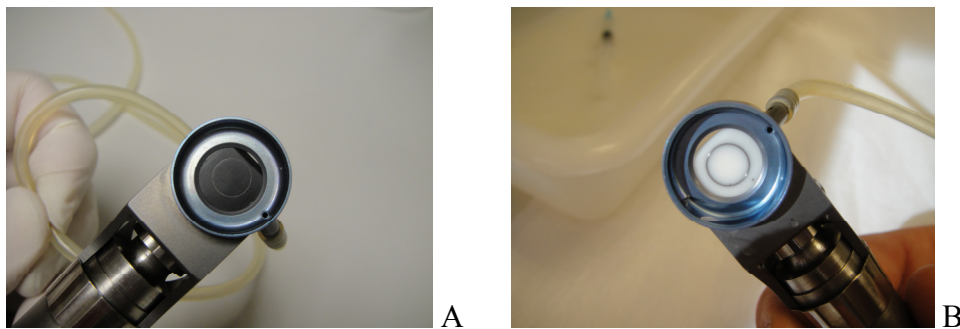


Figure 1 The two 7-mm diameter electrodes with different thickness: 100 μm (A) and 200 μm (B) placed in the applicator based on a modified microkeratome.

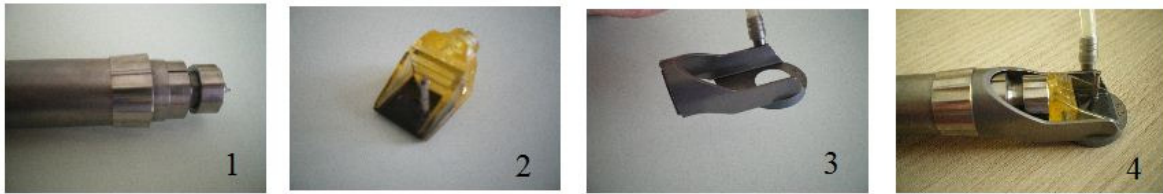


Figure 2 Assembling the microkeratome head. (1) Zone of the handle where the head is located. (2) Head including the epoxy plane (black) in which the circular electrode is embedded. (3) Detail of the head. (4) Assembled applicator inside the microkeratome head and plastic tube for the suction ring.

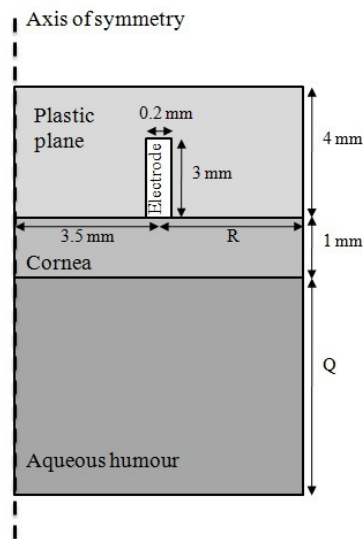


Figure 3 Geometry and dimensions (mm) of the theoretical model. The geometry is mainly divided into four parts: the plastic plane (epoxy plane), the electrode, the cornea and the aqueous humor. Due to the geometry, the problem presented axial symmetry.

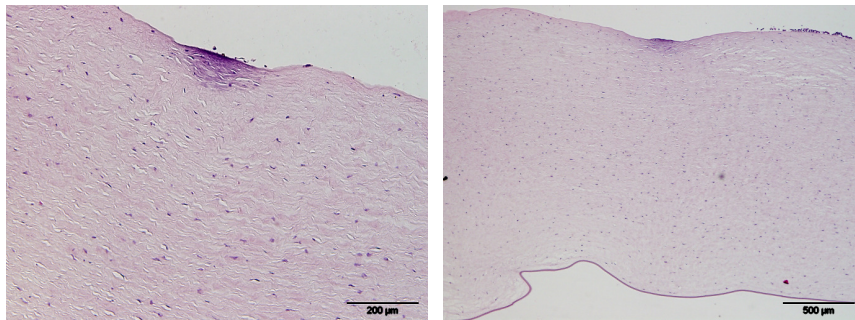


Figure 4 Lesions (H&E) created with the 100 μm electrode in Group 1 (left) and 3 (right). In both cases, lesion depth was no more than 8% of corneal thickness.

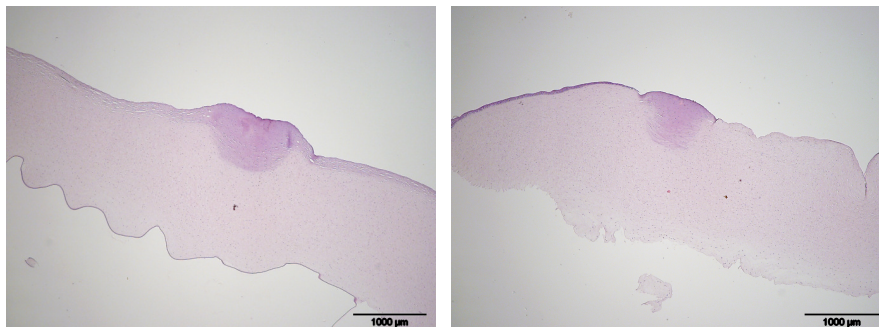


Figure 5 Lesions (H&E) created with the 200 μm electrode in Group 4. In this sample, depth of lesion reached 38% of corneal thickness. Both images are from two sides of the same lesion, indicative of lesion geometry being uniform along the circular path.

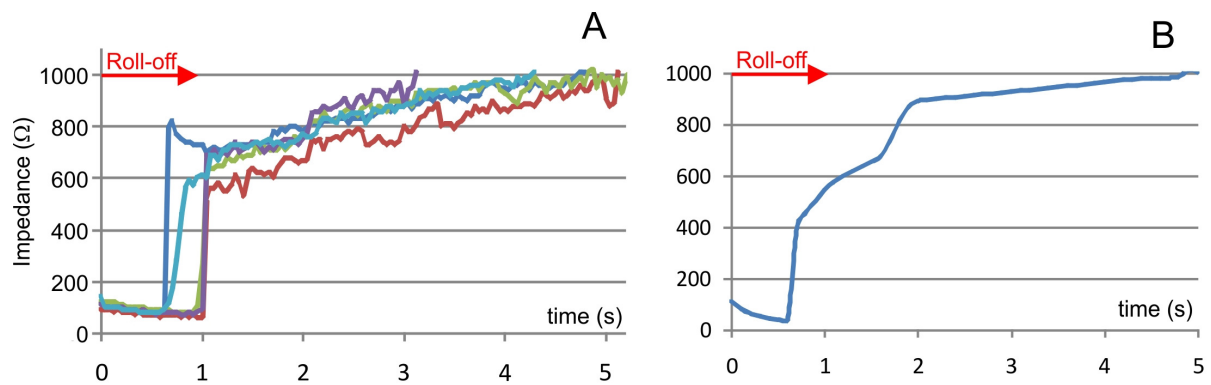


Figure 6 A: Evolution of impedance in the five samples of the Group 4 (50 V up to roll-off, i.e. impedance $>1000 \Omega$). B: Evolution of impedance computed from theoretical model for conditions similar to those of experimental Group 4.

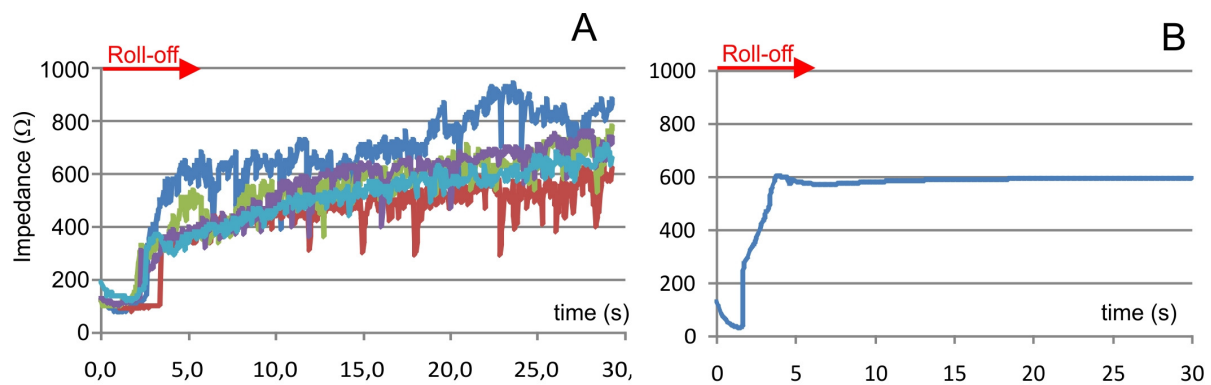


Figure 7 A: Evolution of impedance in the five samples of the Group 5 (30 V, 30 s). No cases of roll off (impedance $>1000 \Omega$) were found. B: Evolution of impedance computed from the theoretical model for conditions similar to those of experimental Group 5.

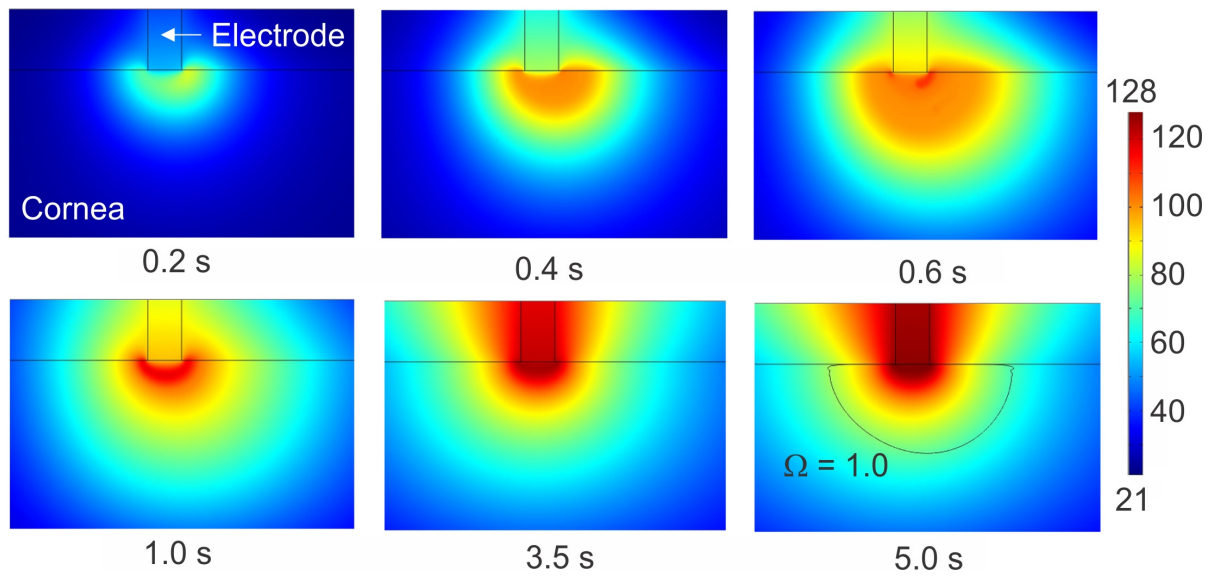


Figure 8 Temperature distributions during RF heating computed for an applied voltage of 50 V for 5 s (similar to conditions in the Group 4 experiments). The $\Omega=1.0$ line indicates the thermal lesion boundary.

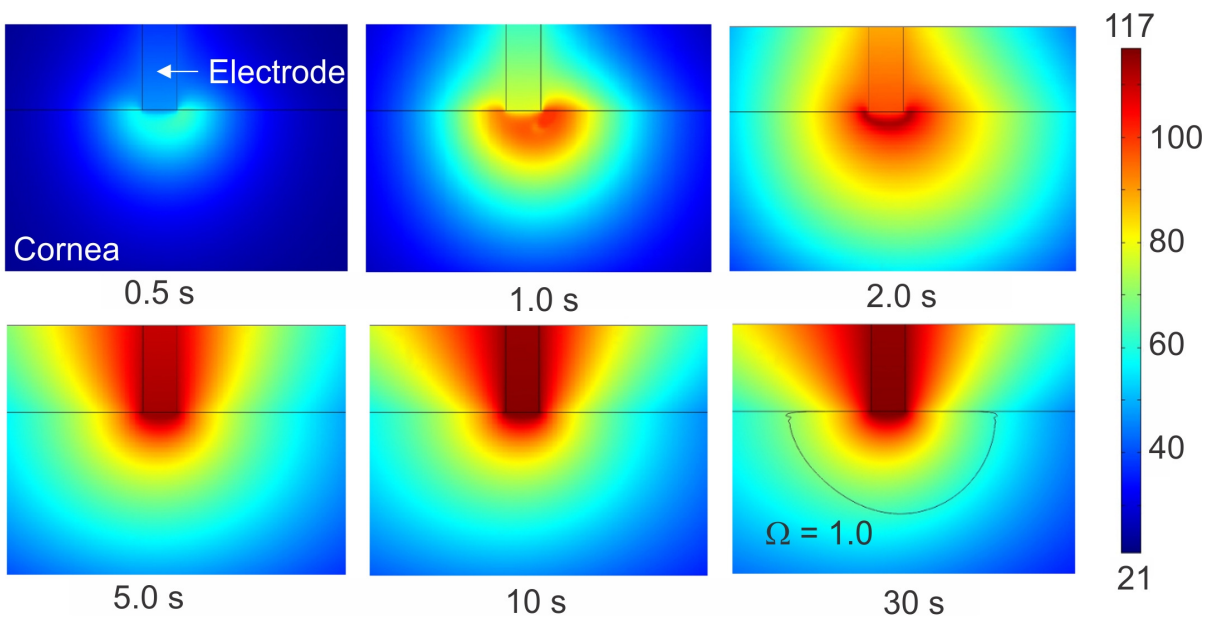


Figure 9 Temperature distributions during RF heating computed for an applied voltage of 30 V for 30 s (similar to conditions in the Group 5 experiments). The $\Omega=1.0$ line indicates the thermal lesion boundary.